Journal of Ocean Engineering and Technology, Vol. 5, No. 2, pp. 171~182, Dec. 1991

⊙ Technical Paper

Design Guidelines of Prismatic Buildings for Antarctic Environment(II)－Snowdrift

Dong-Hyeok Kim*
(*Received October* 12, 1991)

南極環境을 위한 直四角形 建物의 設計指針에 關한 硏究(II)－積雪現況

金 東 爀

Key Words : Antarctic Building(南極建物), Snowdrifting(積雪現像), Similitude Parameters (謨擬 媒介變數), Wind Tunnel Test(風洞實驗), Environmental Control(環境調節), Design Guideline(設計指針)

초 록

南極建物의 機能을 현저히 低下시키는 큰 要因의 하나인 積雪現像에 關한 硏究는 建物로 인한 南極環境에 미치는 人間의 影響(human impact)을 最少化시키기 위한 基本的인 硏究라고 할 수 있다. 南極에 建設될 새로운 建物을 對象으로한 積雪現像의 現地調査나 實物實驗은 여러모로 보아 非經濟的이고 非現實的이기 때문에 風洞實驗의 必要性이 절실해진다. 本 硏究는 積雪現像의 風洞實驗을 위해 必要한 similitude parameters(謨擬 媒介變數)의 重要性 및 各各의 相關性을 分析하였으며 高床式및 地上式의 直四角形의 單獨形 및 group形 建物들 주위에 쌓인 積雪의 形態와 積雪量을 風洞實驗을 通해 調査分析하여 南極建物의 積雪現像에 對한 설계지침(design guideline)을 提示하였다.

1. Introduction

The development of buildings and structures in Antarctica benefits from studies of snowdrifting. Field tests and observations are not only time consuming and expensive, but the necessary environmental control cannot be readily achieved. Although a perfect simulation of snowdrifting has been regarded as extremely difficult to achieve, model testing appears to be the most practical and cost-effective method for investigating snowdrifting problems.

This paper discusses the relevance and signifi-

* Member, Research Associate, School of Civil and Mining Engineering, University of Sydney, N.S.W. 2006, Australia

cance of various similitude parameters for snowdrift modeling. Comparison is made between model and prototype snowdrifts. The results of a series of wind tunnel tests carried out to investigate the snowdrift profiles and volumes for a single building and for groups of buildings, both on-ground and above-ground, are presented.

2. Similarity Criteria for Model Study of Snowdrifting

The similarity requirements for the study of snowdrifting around buildings and structures have been extensively studied by Kind[1,2] Iversen,[3] Anno,[4] Isyumov and Mikitiuk[5] and others. It is generally recognised that it is extremely difficult to fully simulate the behaviour of snow, and at the same time satisfy all similitude criteria at a reduced geometric scale. In particular, the simulation of inter-particle forces, which are mainly dependent on temperature and humidity, is difficult to achieve. To obtain representative results of physical snowdrift modelling, it is required that flow and geometric scale, snow particle cohesiveness and saltation length, snowdrift rate and time scale, and other effects are adequately simulated and properly accounted for when distortion in the scaling proccss becomes necessary.

2. 1 Flow Similarity

Since the physical process of snow particle movement is largely initiated and dominated by a turbulent boundary layer wind, it is believed that the flow characteristics should be properly scaled in addition to other modelling requirements. In the present study, it was necessary to use scales of between 1/50 and 1/100 to produce building models of reasonable size and detail, and to obtain a reasonably sized snowdrifting accumulation. A simulated turbulent boundary layer wind suitable for model scales of 1/50 to 1/100 was generated in a purpose-built Snowdrift Wind Tunnel (Kim et al[6]), essentially modelling a category 2 open country terrain(AS 1170.2−1989[7]). When model snow was introduced, the modified flow characteristics closely resembled those associated with a category 1 exposed open country terrain with a roughness height z_0 close to a prototype value of $0.002m$.

The other relevant atmospheric conditions are :

temperature $= -22.7℃$ for prototype
$= 33℃$ for model

density ρ_a $= 1.324\ kg/m^3$ for prototype
$= 1.193\ kg/m^3$ for model

viscosity ν_a $= 1.206\times10^{-5}\ m^2/s$ for prototype
$= 1.52\times10^{-5}\ m^2/s$ for model

2. 2 Model Particle Selection and Particle Properties

Twelve different particles were tested(Kim et al[6]) for their ability to reproduce the correct snowdrift shape. Commercial standard grade sodium bicarbonate, with a high angle of repose of approximately 90 degrees, was found to produce the most realistic snowdrifting shape. The bulk density ρ_p of sodium bicarbonate was approximately 1300 kg/m^3 and the mean effective diameter D_p was approximately 50 μm. Based on the limited prototype data, a prototype snow density of 700 kg/m^3 and a particle diameter of 150 μm were adopted in this study.

Bagnold[8] proposed the following dimensionless threshold friction speed :

$$A_1 = U_t^* / (\rho_p\ g\ D_p/\rho_a)^{\frac{1}{2}} \quad \cdots\cdots\cdots\cdots\cdots\cdots \quad (1)$$

in which U_t^* is the particle threshold friction speed and g is gravitational acceleration. Based on Equation 1 and the semi-empirical relationships proposed by Iversen et al[7] which included cohesive forces between small particles, the threshold friction speeds were cal-

culated. The terminal fall speed U_f can then be found from $U_f = 2.6\ U_t^*(\text{Feasey}_{10})$. Hence :

$U_{tp}^* = 0.14\ m/s$; $U_{tm}^* = 0.19\ m/s$

$U_{fp} = 0.364\ m/s$; $U_{fm} = 0.494\ m/s$

The estimated prototype threshold friction speed matches well with the value of 0.15 *m/s* suggested by Kind[1] for uncompacted dry snow. The estimated prototype terminal fall velocity also matches reasonably well with the field data presented by Mellor.[11]

2. 3 Geometric Similarity

In addition to model and prototype length scale, it is also necessary to examine the length scale ratio of the model and prototype snow particle size. This particulate geometric similarity can be expressed in the simple form :

$$\frac{D_p}{L} = \text{constant} \quad \cdots\cdots\cdots\cdots\cdots\cdots \quad (2)$$

For a model length scale of 1 to 50 and the respective particle diameters for model and prototype snow, the particulate geometric similarity was not attained. This is a common problem since the ratio D_{mp}/D_{pp} is usually much larger than the ratio L_m/L_p.

2. 4 Similarity of Surface Particle Motion

The behaviour of the particles close to the surface is largely affected by the action of the surface shear stress. A number of similarity requirements have been put forward :

the threshold densimetrical particulate Froude number :

$$\frac{U_t^{*2}}{D_p g}\,\frac{\rho_a}{[\rho_p - \rho_a]} = \text{constant} \quad \cdots\cdots\cdots\cdots \quad (3)$$

the threshold densimetrical geometric Froude number :

$$\frac{U_t^{*2}}{L\ g}\,\frac{\rho_a}{[\rho_p - \rho_a]} = \text{constant} \quad \cdots\cdots\cdots\cdots \quad (4)$$

and,

$$\frac{U^*}{U^*} = \text{constant} \quad \cdots\cdots\cdots\cdots\cdots\cdots\cdots \quad (5)$$

in which U^* is the friction velocity.

2. 5 Similarity of Airborne Particle Motion

Once the particle is airborne and suspended by turbulent diffusion, the similarity of aerodynamic or fluid resistance forces, gravity and inertial effects should be satisfied. A number of similarity requirements have been proposed :

similarity of gravity and fluid forces :

$$\frac{U_f}{U} = \text{constant} \quad \cdots\cdots\cdots\cdots\cdots\cdots\cdots \quad (6)$$

the conventional densimetrical particulate Forude number :

$$\frac{U^2}{D_p g}\,\frac{\rho_p}{[\rho_p - \rho_a]} = \text{constant} \quad \cdots\cdots\cdots\cdots \quad (7)$$

the conventional geometric Froude number :

$$\frac{U^2}{L\ g} = \text{constant} \quad \cdots\cdots\cdots\cdots\cdots\cdots\cdots \quad (8)$$

and similarity of particle and fluid inertia forces :

$$\frac{\rho_p}{\rho_a} = \text{constant} \quad \cdots\cdots\cdots\cdots\cdots\cdots\cdots \quad (9)$$

Kind[2] suggested that an improved similarity of the saltation process is achieved with heavy model snow particles and recommended that $(\rho_p/\rho_a)_m \geq 600$ which was easily satisfied in the present study.

2. 6 Time Scale

Time scaling of snowdrifting is an important similarity requirements in relating experimental

results to prototype conditions. The following dimensionless times have been used :

$$\frac{U\,T}{L} \quad \cdots\cdots (10)$$

$$\frac{\rho_a}{\rho_p}\frac{U\,T}{L} \quad \cdots\cdots (11)$$

$$\frac{1}{2}\frac{\rho_a}{\rho_p}\frac{U^2}{g\,L}\left[1-\frac{U_t}{U}\right]\frac{U\,T}{L} \quad \cdots\cdots (12)$$

in which T is the duration of snowstorm.

Most researchers used a time scale based on one or more or a variation of these dimensionless time formulae. Anno[4] suggested the following equation which was referred to as a dimensionless volume :

$$\frac{T\,Q\,\eta}{\rho_p\,L^2} \quad \cdots\cdots (13)$$

in which Q is the snow drift transport rate, and η is the object's collection coefficient of snow particles which is the weight of accumulated snowdrift divided by the weight of snow particles which pass the object.

3. Significance and Relevance of Snowdrifting Similitude Parameters

The significance and relevance of each parameter was examined for wind tunnel model testing. In particular, snowdrift shapes and volumes obtained in wind tunnel tests were compared with field measurements shown in Figure 1 taken by Mitsuhashi[12] who measured the shapes and accumulated volume of snowdrift around the Observation Hut of the Japanese Shyowa Station in Antarctica. Since the present wind tunnel study was simulating snowdrifting without melting, the data was modified as shown in Fig. 1 to include only those storms or portions of snowstorms which have a positive growth rate. The duration of the modified snowstorms was about 800 hours and the volume of accumulated snowdrift was approximately 90 m^3.

3. 1 Experimental Arrangements

1/50 and 1/100 scale models of the Observation Hut were tested in the Snowdrift Wind Tunnel. Approximately 100 kg of sodium bicarbonate was introduced into the wind tunnel. The internal temperature of the wind tunnel ranged from 27℃ to 37℃ and the relative humidity ranged from 48 % to 65%. The duration of each wind tunnel test run was 4 hours. The wind velocity at a reference height of 10 m in prototype (200 *mm* height at 1/50 model scale and 100 *mm* at 1/100 model scale) at the centre of the working section was maintained at approximately 6 *m/s*.

Contour images of the snowdrift shapes around the model were generated by a grid projection type Moirè fringe camera with a focal length of 1.8 *m*. The size of the area photographed was 900 *mm* × 600 *mm* and the measuring sensitivity was 5 *mm* height. The image was monitored by a closed-circuit television camera. The contour image was captured by a frame grabber, processed and saved on a computer hard disk. The grabbed images were then digitised and processed with contour analysing software which produces three-dimensional perspective or isometric surface representations for output to the TV monitor, printer, or plotter. The program also determined the volume of snowdrift by integration using a trapezoidal rule.

3. 2 Comparison of Model and Prototype Snowdrift

The wind tunnel snowdrift results presented in Figure 2 show a good agreement with the modified prototype data of Mitsuhashi[12] In order to assess how accurately the similarity criteria outlined in Section 2 are being met, the respective 1/

50 scale model and prototype values were determined and are summarised in Table 1.

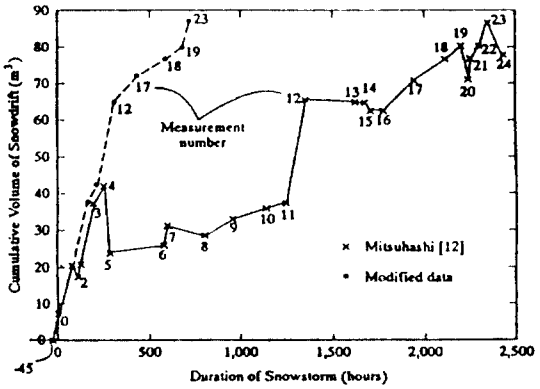

Fig. 1 Original and modified data of Mitsuhashi's[12] prototype snowdrift growth pattern

The similitude requirement of the threshold densimetrical geometric Froude number(Equation 4) shows the biggest mismatch. This mismatch indicates that the model particle trajectory near the surface may be comparatively larger than the prototype snow particle trajectory. Kind[1] suggested that the length of a typical saltation L_s is roughly 10 times its height such that

$$L_s = \frac{10\ U^{*2}}{2\ g} \quad \cdots\cdots (14)$$

The saltation length of the model snow particles under the test conditions was estimated to be approximately 40 *mm* which is smaller than the smallest dimension of the building model and is also considerably smaller than the size of the snowdrift. This has been suggested by Kind[1] to be a desirable feature particularly when proper Froude number scaling was not achieved.

Kind[1,2] also suggested that the similarity of particle forces and particle ejection could be improved if the model roughness height Reynolds number,

$$\left[\frac{U_t^{*3}}{2gv}\right]_m \geq 30 \quad \cdots\cdots (15)$$

Table 1 Model and prototype values of similitude parameters

Eon. No.	Modelling Parameter	Model Value	Proto. Value
2	$\frac{D_p}{b}$	4.2×10^{-4}	2.5×10^{-5}
3	$\frac{U_t^{*2}}{D_p g}\ \frac{\rho_a}{[\rho_p-\rho_a]}$	6.7×10^{-2}	2.5×10^{-2}
4	$\frac{U_t^{*2}}{b\ g}\ \frac{\rho_a}{[\rho_p-\rho_a]}$	2.8×10^{-5}	6.3×10^{-7}
5	$\frac{U^*}{U_t^*}$	1.47	5.7
6	$\frac{U_f}{U}$	8.2×10^{-2}	2.1×10^{-2}
7	$\frac{U^2}{D_p g}\ \frac{\rho_p}{[\rho_p-\rho_a]}$	7.3×10^{4}	1.9×10^{5}
8	$\frac{U^2}{b\ g}$	30.6	4.9
9	$\frac{\rho_p}{\rho_a}$	1090	529
10	$\frac{UT}{b}$	$T_m^{\#}=45$	$T_p^{\#}=800$
11	$\frac{\rho_a}{\rho_p}\ \frac{UT}{b}$	$T_m^{\#}=93$	$T_p^{\#}=800$
12	$\frac{1}{2}\frac{\rho_a}{\rho_p}\frac{U^2}{g\cdot b}\left[1-\frac{U_*}{U}\right]\frac{UT}{b}$	$T_m^{\#}=37$	$T_p^{\#}=800$
13	$\frac{T\ Q\ \eta}{\rho_p b^2}$	$T_m^{\#}=1.5$	$T_p^{\#}=800$

Note : b = width of the Observation Hut
= 6*m* in prototype
unit in *hours*

The value for the present study was 23 which is of similar magnitude to the suggested value.

The similitude requirement of airborne particles based on the conventional densimetrical particulate Froude number (Equation 7) gave a smaller mismatch than the one based on the threshold speed. It appears that the airborne particle behaviour was more accurately simulated than the su-

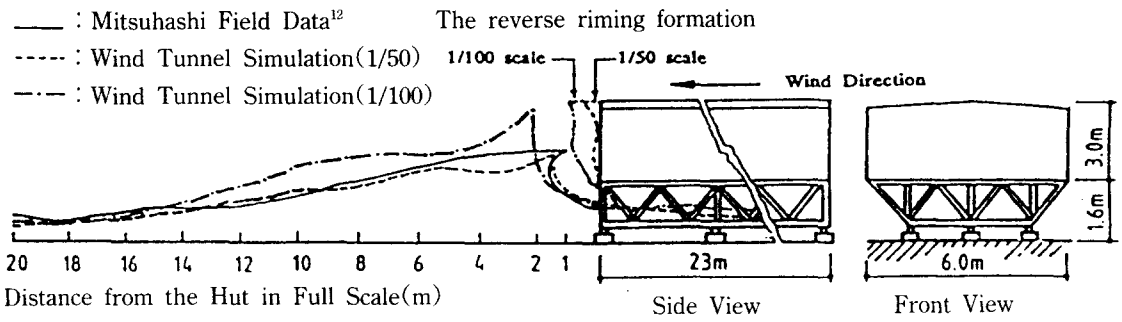

Fig. 2 Snowdrift profiles of prototype, 1/50 and 1/ 100 scale models

rface particle motion. Furhermore, it suggests that turbulent diffusion is a more dominant mechanism than saltation.

Based on a prototype snowstorm duration of 800 hours and an average prototype wind speed of 17 *m/s*, the model snowstorm duration was estimated to be approximately 45 hours, 93 hours and 37 hours respectively according to Equations 10, 11 and 12. Since a good agreement between model and prototype snowdrift shape and volume was achieved after a model test time of 4 hours, time scaling according to Equations 10 and 12 and in particular Equation 11 will lead to conservative snowdrift estimates.

In order to use Anno's[4] dimensionless time scale (Equation 13), the snow drift transport rate has to be estimated for both model and prototype conditions. For the prototype condition, the following drift snow transport rate Q within the layer from 1 *mm* to 300 *m* above the snow surface proposed by Budd et al[13] was used :

$$\log Q_{10}^{300-3} = 1.1812 \times 0.0887\ U_{10} \quad \cdots\cdots\cdots\cdots \quad (16)$$

in which Q is in *g/m.sec*, and U_{10} is the mean wind speed at 10 m height.

The snow drift rate within the 0.6 *m* high working section of the Snowdrift Wind Tunnel, determined by using a vacuum trap system, was found to be 0.19 *kg/m* sec. According to Anno[4], the model snowstorm duration was estimated to be 1.5 hours for a prototype duration of 800 hours. While Anno's[4] time scale produced the closest match between model and prototype time, it will lead to an unconservative estimate.

Inversen's[3] dimensionless time (Equation 12) was used for a more detailed comparison between the model and prototype snowdrift accumulation rates around the Observation Hut. In particular, the progressive snowdrift accumulation and the corresponding wind speed for individual snowstorms shown in the modified prototype data (see Fig. 1) were used in the analysis. The progressive snowdrift accumulation rate normalised by

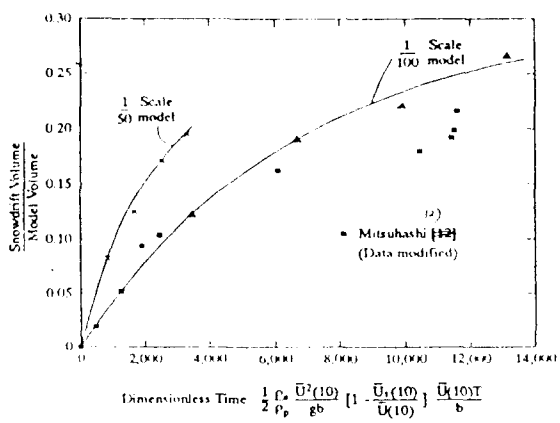

Fig. 3 Snowdrift growth patterns of prototype, 1/ 50 and 1/100 scale models

the building volume is expressed as a function of dimensionless time in Figure 3. It can be seen that there is a reasonably good agreement between the results for the 1/100 scale model and the prototype. For the 1/50 scale model, time scaling according to Iversen's dimensionless time will produce a conservative estimate of snowdrift volume. Nevertheless, a test model at 1/50 scale is often necessary due to the relatively small size of buildings and structures usually found in Antarctica.

4. Snowdrifting Around Prismatic Buildings

Models of prismatic buildings were tested in the Snowdrift Wind Tunnel according to the experimental procedure described in Section 3.1. The building models used were based on the dimensions of a 56 *mm* high (h_1) by 72 *mm* wide (b_1) by 120 *mm* long (l_1) rectangular prism which represents a module similar to a shipping container at 1/50 scale.

The first series of tests was carried out on a single building, both on-ground and above-ground. Three above-ground configurations were tested : h_2=18 *mm* (0.9 *m* in prototype), 24 *mm* (1.2 *m*) and 30 *mm* (1.5 *m*) above ground which represented relative heights above ground h_2/h_1 of 0.32, 0.43 and 0.54, respectively. The wind angle was maintained at a right angle to the short axis (b_1) of the models as shown in Fig. 4(i).

The second series of tests was carried out on a group of three identical buildings, both on-ground and above-ground, with varying distance (b_2) between them and for a wind angle at a right angle to the long axis(l_1) of the model, as shown in Fig. 4(ii). Three relative separations were tested : b_2/b_1 above =0.33, 0.5 and 1. For the above-ground configurations, a relative height avove ground h_2/h_1 of 0.32 was used.

4.1 Experimental Results

4.1.1 Snowdrift around Single On-ground and Above-ground Buildings

The isometric views, and side and front views of the snowdrift formations around the single on-ground and above-ground buildings at the end of four hours testing period are presented in Tables 2 and 3 respectively. The growth rates of the snowdrifts are presented in Figure 5 in which the snowdrift volume normalised by the single building model volume is plotted against the dimensionless time. It can be seen that the snowdrift volumes for the on-ground building and for the h_2/h_1=0.32 elevated building are very similar. As the building was elevated to a higher position, the snowdrift volume was reduced considerably. It is important to note that for the on-ground building, the snowdrift was attached to the leeward side of the building. This often creates problems in the building's design including the blockage of entrances and windows and additional snow loading on the leeward wall of the building. While the h_2/h_1 =0.32 elevated building did not reduce the snowdrift volume, the snowdrift was formed well clear of the leeward wall. Although the other two

Table 2 Isometric views of snowdrift formations around a single building

Height	Snowdrift Shape
h_1 h_2 On-ground	Direction of wind 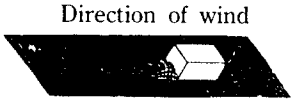
h_2/h_1=0.32	
h_2/h_1=0.43	
h_2/h_1=0.54	

more highly elevated buildings created considerably smaller snowdrifts, the additional height will increase the wind-induced loads on and reduce the stiffness of the buildings which in combination will increase building vibrations. This should be taken into account in the structural design of the building, in particular in the design of supports for elevated buildings.

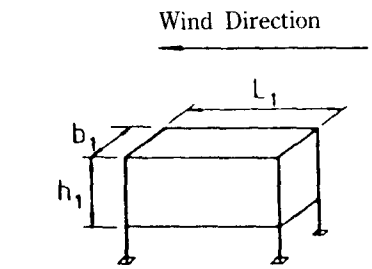

(i) Single building

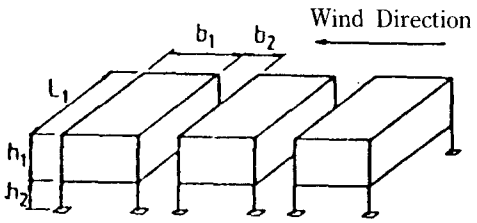

(ii) A group of three buildings

Fig. 4 Experimental arrangements

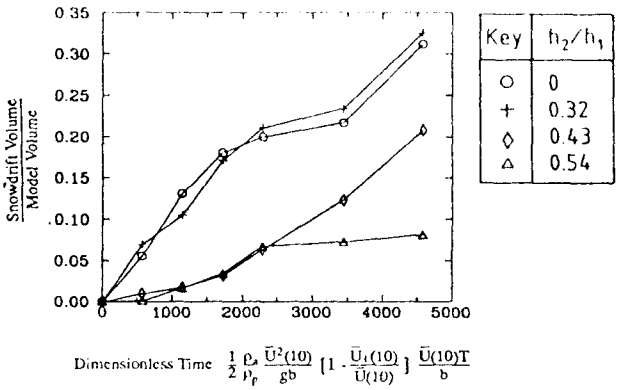

Fig. 5 Snowdrift growth patterns for a single building

4.1.2 Snowdrift around Grouped On-ground and Above-ground Buildings

The side views of the snowdrift formations around the grouped on-ground and above-ground buildings at the end of the four hour testing period are presented in Table 4. The growth rates of the snowdrifts are presented in Fig. 6.

Table 2 Side and front views of snowdrift formation around a single building

Height	Side View	Front View
On-Ground		
$h_2/h_1=0.32$	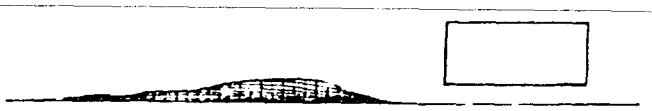	
$h_2/h_1=0.43$	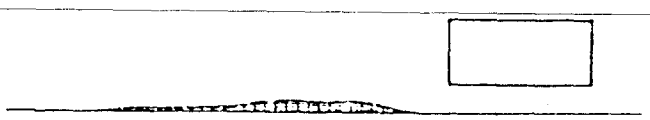	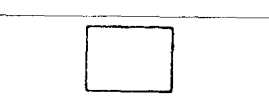
$h_2/h_1=0.54$	Direction of Wind 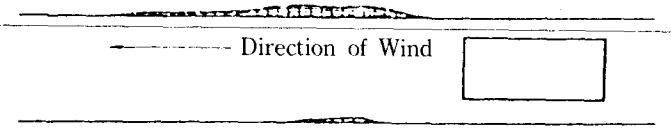	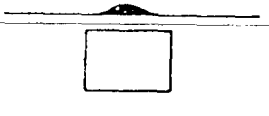

Key	b_2/b_1	h_2/h_1
●	0.33	0
■	0.5	0
△	1.0	0
○	0.33	0.32
□	0.5	0.32
△	1.0	0.32

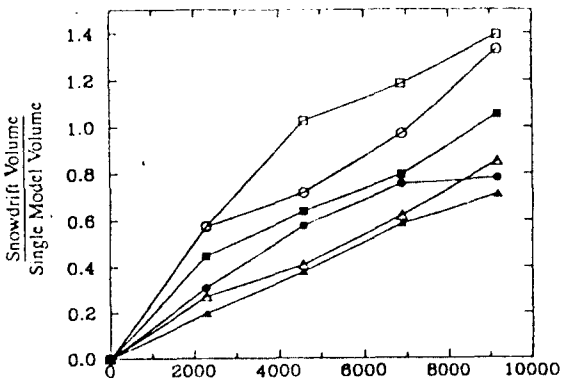

Fig. 6 Snowdrift growth patterns for groups of buildings

For the grouped on – ground buildings, the bulk to the snowdrifts formed at the lee of the last building in the group and the snowdrift was attached to the leeward wall. In addition, significant snowdrifts formed between buildings and were attached to neighbouring walls, with the largest snowdrifts forming for a relative separation $b_2/b_1 = 0.5$. A relative separation $b_2/b_1 = 0.5$ also produced the largest total snowdrift volume. For a relative separation $b_2/b_1 = 1$, the amount of snowdrifts forming between buildings was greatly reduced. Both the attached leeward snowdrifts and the snowdrifts between buildings will create the same kind of design problems as those discussed earlier.

For the grouped above – ground buildings, the bulk of the snowdrifts were also formed at the lee of the last building in the group, but the snowdrifts were not attached to the leeward wall. In sharp contrast to the grouped on – ground buildings, there was virtually no snowdrift between and underneath the buildings for a relative separation $b_2/b_1 = 0.33$. However, such snowdrift formation became more noticeable as the relative separation $b_2/b_1 =$ increased, but the snowdrift remained too small to come into contact with any part of the buildings, up to a relative separation $b_2/b_1 = 1$. The total snowdrift volume decreased as the relative separation $b_2/b_1 =$ increased. For the same relative separation b_2/b_1, the total snowdrift volumes for the above – ground configurations were larger than for the corresponding on – ground buildings.

It is noted that the snowdrift formations around both the grouped on – ground and above – ground buidings were dependent on the relative separation between buildings and there is expected to be a separation limit above which the interaction between buildings will disappear. At that point, each building forming a group is expected to behave effectively as a single building and create its own snowdrift accordingly.

Table 5 shows the top views of the reversed riming formation at the leeward side of the last building of the group. the largest riming formation was observed for the grouped above – ground buildings with a relative separation $b_2/b_1 = 0.33$. It is interesting to observe the riming formation for the grouped on – ground buildings displayed a single peak in the middle and two horn – shaped formations at the corners. For the grouped above – ground configurations, there were two peaks for relative separations $b_2/b_1 = 0.33$ and 0.5, while there was no peak for a relative separation $b_2/b_1 = 1$ except for two horn – shaped formations at the corners. The cause of these riming formations is unknown but is believed to be closely re-

lated to the different flow characteristics associated with the different building configuration.

Table 4 Side views of snowdrift formations around groups of buildings

	b_2/b_1	Side View
On-Ground	0.33	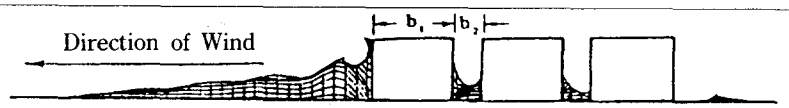
	0.5	
	1	
Above-ground	0.33	
	0.5	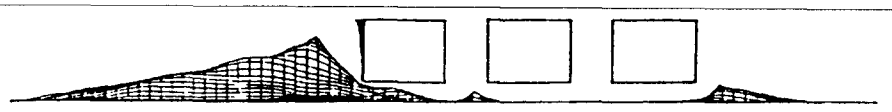
	1	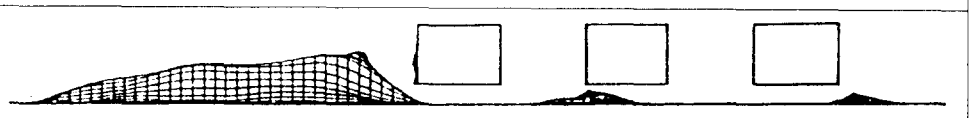

Table 5 Top views of riming formations

	b_2/b_1 = 0.33	b_2/b_1 = 0.5	b_2/b_1 = 1
ON-GROUND	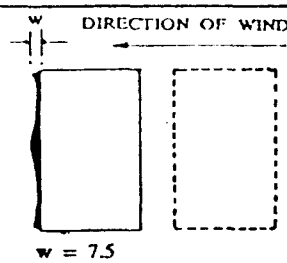	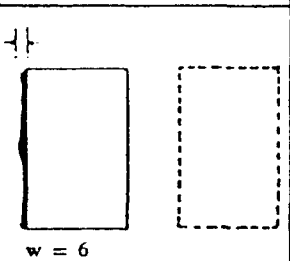	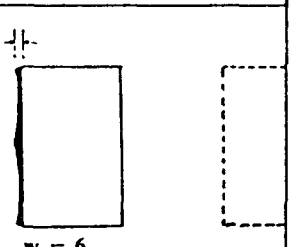
ABOVE-GROUND	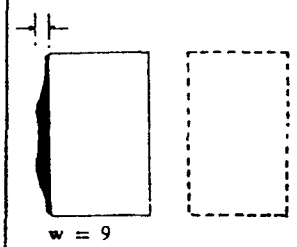	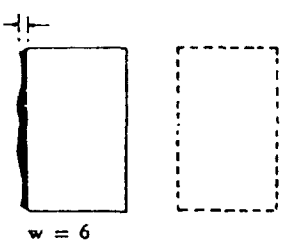	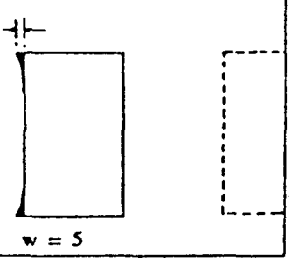

Notes : w is the maximum width (in *mm* model scale) of the riming formation.

5. Conclusions

1) There were good agreements between model and prototype snowdrift shapes despite mismatches in both the threshold densimetric and conventional Froude number scalings shown in Table 1, Therefore, it confirm the general belief that strict Froude number scaling can be relaxed in simulating snowdrift phenomena. It also appears that turbulent diffusion could be a more dominant mechanism than saltation.

2) Time scaling is an important similitude paramenters for the prediction of snowdrift accumulation. Iversen's[3] proposed dimensionless time (Equation 12), which includes particle and fluid densities, Froude number, particle threshold speed, mean wind speed, time and length, produced a reasonable correlation between model and prototype snowdrift accumulation rates.

3) For a single on－ground building, the snowdirft was attached to the leeward side of the building which often creates problems in the building's design. By elevating the building, snowdrift can be substantially reduced and forms well clear of the building. The wind load and vibration of elevated buildings should be taken into account in the structural design of the building, in particular in the design of supports for elevated builings.

4) For grouped on－ground buildings, a large snowdrift formed at the lee of the last building and was attached to the leeward wall. Significant snowdrifts also formed between buildings and were attached to the neighbouring walls. Although grouped above－ground buildings created larger snowdirfts compared to the corresponding grouped on－ground buildings, the snowdrifts were not attached to the leeward wall and there was comparatively little snowdrift forming between and underneath the buildings.

Acknowledgements

This work was supported by a grant from the Australian Research Grant Scheme awarded to Associate Professor Kwok and Mr. Rohde. The efforts of Mr. Brew and Miss Pham in tracing graphs and tables are acknowledged.

References

1) Kind, R.J., "A Critical Examination of the Requirements for Model simulation of Wind Induced Erosion Deposition Phenomena such as Snow Drifting", Atmos. Environ., Vol. 10, pp. 219－227, 1976

2) Kind, R.J., "Snowdrifting : A Review of Modelling Methods", Cold Regions Science and Technology, Vol. 12, pp. 217－228, 1986

3) Iversen, J.D., "Drifting Show Similitude－Drift Deposit Rate Correlation", Proc. Int. Conf. on Wind Engineering, Ft. Collins, Colorado, Permagon Ltd., pp. 1037－1080, July 19 79

4) Anno, Y., "Requirements for Modelling of Snowdrift", Cold Regions Science and Technology, Vol. 8, pp. 241－252, 1984

5) Isyumov, N., and M. Mikitiuk, "Wind Tunnel Model Tests of Snow Drifting on a Two－Level Flat Roof", Proceedings of the 6th U.S. National Conference on Wind Engineering, University of Houston, Texes, Vol. II, pp. A6

-47 to A6-58, 1989

6) Kim, D.H., K.C.S. Kwok and H.F. Rohde, "Wind Tunnel Model Study of Antarctic Snowdrifting", Proceedings of 10th Australasian Fluid Mechanics Conference, Univ. of Melbourne, Vol. 2, pp. 9.35-9.38, 1989

7) Australian Standard, SAA Loading Code Part 2 : Wind loads, As 1170.2-1989

8) Bagnold, R.A., "The Physics of Blown Sand and Desert Dunes", Methuen, London, 1941

9) Iversen, J.D., R. Greeley and J.B. Pollack, "Windblown Dust on Earth Mars and Venus", J. Atmos. Sci., Vol 33, pp. 2452-2429, 1976

10) Feasey, R. "Wind Tunnel Studies of Snow Deposition at Scott Base", Central Res. Rep. No. 9-80/1, Ministry of Works, Lower Hutt, New Zealand, 1980

11) Mellor, M. "Blowing Snow", Cold Region Sciences and Engineering, Part III, A3C, U.S. Army Cold Regions Research and Engineering Laboratory, Hampshire, 1965.

12) Mituhashi, H., "Measurements of Snowdrifts and Wind Profiles around the Huts of Showa Station in Antarctica", Antarctic Record, No. 75, pp. 37-56, 1982

13) Budd, W.F., R.J. Dingle and U.Radok, "The Byrd Snow Drift Project : Outline and Basic Results", Antarctic Research Series, American Geophysical Union, Vol. 9, pp. 71-134, 1966